Characterisation of nonlinear aeroservoelastic behaviour

G. Dimitriadis & J. E. Cooper
School of Engineering
University of Manchester
Oxford Road, Manchester M13 9PL
United Kingdom
mbgssgd2@fs1.eng.man.ac.uk
jecooper@man.ac.uk

Abstract

The characterisation of the behaviour of nonlinear aeroelastic systems has become a very important research topic. Nevertheless, most of the work carried out to date concerns the development of unsteady CFD solutions in the transonic region. Important though this work is, there is also a need for research which aims at understanding the behaviour of nonlinear systems, particularly the occurance of Limit Cycle Oscillations (*LCOs*). The purpose of this paper is to study the stability of a simple aeroservoelastic system with nonlinearities in the control system. The work considers both structural and control law nonlinearities and assesses the stability of the system response by use of bifurcation diagrams. It is shown that simple feedback systems designed to increase the stability of the linearised system also stabilise the nonlinear system, although their effects can be less pronounced. Additionally, a nonlinear control law designed to limit the control surface pitch response was found to increase the flutter speed considerably by forcing the system to undergo limit cycle oscillations instead of fluttering. Finally, friction was found to affect the damping of the system but not its stability, as long as the amplitude of the frictional force is low enough not to cause stoppages in the motion.

1 Introduction

Over the past two decades there has been a pronounced increase in research into nonlinear aeroelasticity. It has been known for quite some time that aircraft contain a number of nonlinearities which can significantly affect vibratory characteristics. These nonlinearities give rise to phenomena (e.g. Limit Cycle Oscillations (LCO)) that cannot occur if the system is linear. Consequently, it is impossible to model and predict such behaviour using a linear analysis. This limitation is becoming of increasing importance with the latest generations of aircraft.

Some early work on nonlinear aeroelasticity [1] showed that limited amplitude oscillations in aircraft are nonlinear phenomena. Breitbach [2] identified a number of sources of nonlinearity in aircraft such as kinematic deflections of control surfaces, solid friction in hinge bearings as well as distributed nonlinearities due to elastic deformations in riveted, screwed and bolted connections. Since then, several investigations of nonlinear aeroelastic behaviour have been conducted, most of which concentrated on structural and aerodynamic nonlinearities. The whole area of prediction and characterisation of LCO has been defined as being an area of critical research interest [3]. However, most work has concentrated upon the development of unsteady CFD solutions [4] primarily in the transonic region. Some recent notable exceptions are the experimental work carried out by Holden et al [5] and Conner et al [6] as well as various numerical studies such as [7].

The increasing power of modern computers allowed the use of increasingly computationally intensive mathematical tools for the characterisation of nonlinear behaviour, such as bifurcation plots [8] and parameter-space sections [9]. Limit Cycle Oscillations (*LCOs*) have been observed and explained in terms of Hopf bifurcations [10] and the possibility of LCO control and suppression has been investigated [11], [12]. However, the main subject of all this research has been structural nonlinearities and, to a lesser extent, aerodynamic nonlinearities [13]. Little research has been conducted into the effects of nonlinearities in the control system even though, with the advent of Active Control Technology (*ACT*), control systems are becoming increasingly nonlinear. Aeroservoelasticity [14] is a relatively recent research topic which is generally dominated by case studies such as [15].

Stability is of paramount importance in the design of all control systems whether they be linear or nonlinear. However, the performance of nonlinear aeroservoelastic systems throughout the desired flight envelope as well as their interaction with non-designed nonlinearities, such as backlash in the linkage elements of the control system, has not been thoroughly investigated.

In this paper, the aeroservoelastic behaviour of a number of simulated systems is investigated and characterised. The purpose of the work is to give an overview of possible nonlinear behaviour that may occur either near flutter, or as a result of the interaction of the control system with structural nonlinearities. Partricular emphasis is given to assessing whether control laws designed to improve the stability of linear systems also have a stabilising influence on nonlinear systems. The simulated systems

Paper presented at the RTO AVT Specialists' Meeting on "Structural Aspects of Flexible Aircraft Control", held in Ottawa, Canada, 18-20 October 1999, and published in RTO MP-36.

considered contain a variety of nonlinearities that can occur in the control system, ranging from nonlinear springs in the control actuator to nonlinear control laws.

2 Simulated aeroservoelastic systems

The basis of all the systems investigated in this work is an extension of the Hancock aeroelastic model [16]. The basic Hancock model is a rigid wing with two springs at the wing root, giving the system two degrees of freedom, heave and pitch. The aerodynamics is modelled using quasi-steady strip theory with approximate unsteady aerodynamic derivatives. The model used here also includes a control surface [12], i.e. it incorporates an additional degree of freedom. The control surface is driven by a Power Control Unit (*PCU*) or Power Actuator. The PCU provides both stiffness and structural damping. The basic simulated system, which is shown in figure 1, was modified by the addition of a number of nonlinearities giving rise to four different systems, with two possible control laws.

2.1 Bilinear PCU spring

The Power Control Unit contains a pressure feedback spring, as shown in figure 2. The first system examined in this paper has a bilinear pressure feedback spring. Bilinear stiffness is a piecewise linear function shown in figure 3. The stiffness, K_1, in the inner region (delimited by $\pm\delta$ in figure 3) is lower than the stiffness in the outer region, K_2.

This is not a straightforward case of bilinear stiffness in the control surface since, because the bilinear spring is in the PCU, it affects the control surface velocity as well as displacement. The PCU equation is

$$\frac{VK_F}{4N}\dot{P}_J + K_V A_F \sqrt{P_s/2} P_J = dK_F A_P \dot{\beta} + \mu d K_F K_V \sqrt{P_s/2}\beta - \mu d K_F K_V \sqrt{P_s/2}\beta_i \quad (1)$$

where V is the volume of the PCU, N is the bulk modulus of oil, P_J is the difference of pressures in the two PCU compartments P_1 and P_2 (see figure 2), K_V is a valve flow constant, A_F is the effective area of the pressure sensing chamber, P_s is the supply pressure, K_F is the stiffness of the pressure feedback spring, μ is the lever arm ratio, d is the distance between the PCU axis and the wing chord, β is the control surface deflection and β_i is the demand angle. It can be seen that K_F multiplies both the $\dot{\beta}$ and β terms. Hence, a nonlinear pressure feedback spring affects both control surface velocity and displacement.

2.2 Freeplay in PCU spring

In this case, the pressure feedback spring contains freeplay. Freeplay stiffness is also a piecewise linear function, depicted in figure 4. In this case, the stiffness in the inner region is zero. Again, the freeplay affects both control surface velocity and displacement.

2.3 Backlash in PCU spring

Backlash is a piecewise linear hysteretic nonlinearity. Figure 5 shows the variation of the force in the PCU with control surface deflection during a Limit Cycle Oscillation, in the presence of backlash in the pressure feedback spring. Whenever the control surface pitch changes direction, the force in the PCU jumps from one of the sloped lines to the other. The horizontal distance between the two branches is called the backlash distance. Such behaviour can be observed for example in the bearings of all-movable control surfaces of military aircraft [17]. In the american literature backlash is sometimes referred to as freeplay however, in this paper, the terms backlash and freeplay denote two distinct types of nonlinearity.

As with bilinear stiffness and freeplay, backlash affects both the velocity and displacement of the control surface of the system investigated here.

2.4 Friction in PCU

This case models friction between the piston seals and the chamber. The friction depends on the piston velocity, hence the force, F, in the piston is given by

$$F = A_p P_J + F_R \text{sgn}(\dot{\beta}) \quad (2)$$

where F_R is the magnitude of the friction force. Generally, it was assumed that F_R was low enough to allow movement of the piston without stoppages.

2.5 Delayed Feedback

A displacement feedback loop was added to the linear system, in order to increase the separation of the natural frequencies. The feedback gains were calculated such that the separation of the two closest natural frequencies was increased by 20%. The changes in the natural frequencies at a speed of 40m/s are tabulated in table 1

Open Loop	Closed Loop
37.2441 Hz	46.3668 Hz
14.3522 Hz	15.2619 Hz
8.7812 Hz	8.4752 Hz

Table 1: Open and closed-loop natural frequencies of linear system at V=40m/s

A further consequence of the displacement feedback was that the flutter speed of the linear system was increased by 1.9%. Figures 6 and 7 show the open and closed loop natural frequencies and dampings respectively for a range of airspeeds. The open loop eigenvalues were obtained by direct solution of the system equations of motion while the eigenvalues of the closed loop system were calculated by curve-fitting the impulse response, hence

they look less smooth. The figures show that all the natural frequencies of the closed-loop system are more separated than those of the open loop system and that, even though the damping of the critical degree of freedom in the closed loop system is lower, the closed loop flutter speed is higher than that of the open loop system.

To simulate the fact that real control systems do not act spontaneously, the feedback signal was delayed by $n\Delta t$ seconds, where n can be varied. The delayed feedback control system was also used in conjunction with the freeplay, bilinear, backlash and friction nonlinearities mentioned above.

2.6 Control Surface pitch limit

An active control system was devised to limit the control surface pitch. Initially, it was assumed that the control system knows at all times the exact value of the control surface pitch. The pitch, β, at time t is used in conjunction with the value of the pitch at time $t - \Delta t$ to predict $\beta(t + \Delta t)$ using linear curve-fitting, i.e.

$$\beta(t + \Delta t) = 2\beta(t) - \beta(t - \Delta t)$$

If $\beta(t + \Delta t)$ exceeds a given limit, β_{lim}, then the control system feeds back $-K\beta$ through the actuator, where K is some constant. Since a real control system would not be able to instantaneously complete all the calculations, acquire the current value of β and feed it to the actuator, the feedback in the simulated system is delayed by Δt.

3 Limit Cycle Oscillations and bifurcation diagrams

For a single degree-of-freedom system, a Limit Cycle Oscillation (*LCO*) is a limited amplitude oscillation occurring around a line singularity in the phase-plane called a limit cycle. Such a limit cycle can be seen in figure 8. The figure plots velocity ($\dot{\beta}$) against displacement (β) for a system undergoing LCO. The resulting curve is the limit cycle. Limit cycles are singularities since they can either attract the phase trajectories (stable limit cycle) or repel them (unstable limit cycle). In the case of figure 8, where a stable limit cycle is shown, the system response will always wind onto the limit cycle both from the inside and from the outside. In turn, this signifies that the limit cycle cannot be crossed. A limit cycle can be classed as period-1, period-2, etc depending on its complexity. Figure 8 shows a limit cycle with only one loop, i.e. period-1. A period-3 limit cycle, with three loops, can be seen in figure 9.

For a multiple degree-of-freedom system, a limit cycle is a multi-dimensional singularity, its dimensions being equal to the number of states in the system. However, limit cycles can still be visualised using phase-plane plots of the type shown in figures 8 and 9, provided the velocity and displacement for the same degree-of-freedom (or mode) is plotted. In the case of aeroelastic systems, whose behaviour changes with airspeed, phase-plane plots are not sufficient to determine their stability. To this purpose it is necessary to use bifurcation plots, which can track the stability of a system over any range of airspeeds. Bifurcation plots can be constructed by obtaining the impulse response of a system and then calculating the displacement of one of the degrees of freedom when the velocity of the same degree of freedom is zero. If the system is undergoing a limit cycle at a particular velocity, then the values of the displacement will be repeated. For example, in the case of figure 8, when, the displacement takes two values at zero velocity. In figure 9, there are six possible values of the displacement at zero velocity. A bifurcation plot is obtained when all the values of the displacement when the velocity of that DOF is zero are plotted against airspeed.

Figure 10 shows a bifurcation plot for the system with bilinear pressure feedback spring described earlier. For airspeeds where the system is stable (up to 45 m/s), only zeros are plotted. Between 45 m/s and just over 52 m/s, the system undergoes LCOs. The limit cycles are period-1, hence there are only two points plotted at each airspeed. The amplitudes of the limit cycles increase almost linearly up to approximately 51 m/s. Between 51 and 52 m/s, the amplitudes increase exponentially, which is a sign that the system is close to instability. At speeds above 52 m/s, the system becomes completely unstable and flutters.

4 Stability of the Aeroservoelastic Systems

The impulse response of the non-linear systems described in section 2 were calculated for a range of different airspeeds. Bifurcation plots were then generated in order to characterise the Limit Cycle behaviour.

4.1 Stability of Bilinear System

As mentioned already, figure 10 is the bifurcation plot for the system with bilinear pressure feedback spring. There are three distinct regions of stability, tabulated in table 2.

Airspeed (m/s)	Stability
< 45.2	Stable
45.2-52.2	Period-1 Limit Cycle
> 52.2	Unstable (flutter)

Table 2: Stability of bilinear system

Systems with bilinear systems have already been extensively analysed in previous work such as reference [18]. The purpose of this section is to investigate the effects of bilinearity in conjunction with control action to the stability of an aeroservoelastic system. Hence, results are presented from the coupling of the bilinear system with the displacement feedback of section 2.5. It has already been

mentioned that the displacement feedback system was designed to stabilise the linear aeroservoelastic system. The two main considerations in this section are whether the feedback system can also stabilise the bilinear system and also what are the effects of delaying the feedback. It is of interest to note that the system with bilinear stiffness undergoes LCOs at airspeeds above the flutter speed of the linear system with stiffness K_1 and below the flutter speed of the linear system with stiffness K_2.

Figure 11 shows the bifurcation diagram for the bilinear system with feedback (not delayed). It can be seen that LCOs only begin to occur at airspeeds higher than 49 m/s. Additionally, up to approximately 51.5 m/s the amplitudes of the limit cycles are very low. Flutter occurs at 54 m/s. The stability of the system is summarised in table 3

Airspeed (m/s)	Stability
< 49	Stable
49-54	Period-1 Limit Cycle
> 54	Unstable (flutter)

Table 3: Stability of bilinear system with undelayed feedback

Consequently, the effect of the feedback was to stabilise the system, despite the bilinear actuator spring. Limit cycles appear later than in the open loop system and they are of lower amplitude. Additionally, flutter is delayed by approximately 3%.

Delaying the feedback signal by one simulation timestep has an adverse effect on the stability of the closed-loop system. Figure 12 shows the bifurcation diagram for the bilinear system with delayed feedback. Limit cycles (period-1) first appear at 46 m/s but their amplitudes remain low up to an airspeed of just over 48 m/s. At 51 m/s, the limit cycles change to period-3. Finally, at 52.5 m/s the system starts to flutter. Table 4 summarises the information from figure 12.

Airspeed (m/s)	Stability
< 46	Stable
46-51	Period-1 Limit Cycle
51-52.5	Period-3 Limit Cycle
> 52.5	Unstable (flutter)

Table 4: Stability of bilinear system with delayed feedback

Nevertheless, the system with delayed feedback is more stable than the open-loop system since limit cycles appear later and are initially of much smaller amplitude.

4.2 Stability of freeplay system

As with bilinear stiffness, freeplay has been already thoroughly investigated, most recently in [7] and [6]. Here, the effect of freeplay in conjunction with displacement feedback is of interest. Firstly, it should be mentioned that freeplay is a much more nonlinear function than bilinear stiffness and that its effects are more pronounced. With the reference to the system investigated here, it should be noted that, since the stiffness is zero inside the freeplay region, the only source of stiffness in the control surface pitch direction is aerodynamic stiffness. This in turn signifies that LCOs are expected to be encountered at lower airspeeds than in the bilinear system.

Figure 13 is the bifurcation plot for the system with freeplay in the pressure feedback spring but no feedback. The first limit cycles appear at 19m/s and they are period-2. At approximately 33m/s the limit cycles change to period-1. Finally, the system flutters at 52m/s (see table 5).

Airspeed (m/s)	Stability
< 19	Stable
19-33	Period-2 Limit Cycle
33-52	Period-1 Limit Cycle
> 52	Unstable (flutter)

Table 5: Stability of freeplay system without feedback

Figure 14 shows the bifurcation diagram for the freeplay system with undelayed feedback. The system is stable up to an airspeed of 20m/s when period-3 limit cycles appear. The amplitude of the limit cycles increase slowly until 53m/s when the system begins to undergo period-4 LCOs. Finally, flutter occurs at 55 m/s. The stability summary in table 6 shows that the feedback has stabilised the system by delaying the appearance of LCOs by 1m/s and delaying flutter by 3m/s. Additionally, the amplitudes of all limit cycles are lower than in the open loop system. However, the stabilisation is not as radical as it was with the bilinear system.

Airspeed (m/s)	Stability
< 20	Stable
20-53	Period-3 Limit Cycle
53-55	Period-4 Limit Cycle
> 55	Unstable (flutter)

Table 6: Stability of freeplay system with undelayed feedback

Finally, figure 15 shows the bifurcation diagram for the freeplay system with delayed feedback. Limit cycles first appear at 20m/s and are period-3, as with the undelayed feedback however, in this case there are no period-4 LCOS. Flutter occurs at 53m/s.

Airspeed (m/s)	Stability
< 20	Stable
20-53	Period-3 Limit Cycle
> 53	Unstable (flutter)

Table 7: Stability of freeplay system with delayed feedback

Figure 15, as well as table 7, show that the main effect

of the delay is to decrease the flutter airspeed. Nevertheless, as with the bilinear case, the delayed feedback system is more stable than the open loop system since flutter occurs 1m/s later and the limit cycles have smaller amplitudes.

4.3 Stability of system with backlash

Figure 16 is the bifurcation plot for the open-loop system with backlash in the pressure feedback spring. The system is stable up to an airspeed of 44m/s when very low amplitude period-1 limit cycles appear. At approximately 51.5m/s the system flutters (see table 8). Hence, backlash decreases the flutter velocity of a system and introduces small amplitude limit-cycles at the high subcritical airspeed range.

Airspeed (m/s)	Stability
< 44	Stable
44-51.5	Period-1 Limit Cycle
> 51.5	Unstable (flutter)

Table 8: Stability of backlash system without feedback

Figure 17 displays the bifurcation diagram for the system with backlash in the pressure feedback spring and undelayed feedback. Again, the first limit cycles appear at 44m/s and are low amplitude period-1. However, flutter is delayed beyond the flutter airspeed of the linear system by high amplitude period-1 LCOs in the range 52.5-53.5m/s. After 53.5m/s continuous bifurcations to higher period limit cycles occur. Such behaviour is termed period-doubling [12] and is an indication of imminent instability either to flutter or to chaotic behaviour. In this case period-doubling leads to flutter at 53.8m/s.

Airspeed (m/s)	Stability
< 44	Stable
44-52.5	Low amplitude Period-1 Limit Cycle
52.5-53.5	High amplitude Period-1 Limit Cycle
53.5-53.8	Period doubling
> 53.8	Unstable (flutter)

Table 9: Stability of backlash system with feedback, no delay

Finally, figure 18 shows the bifurcation diagram for the backlash system with delayed feedback. The behaviour of the system is identical to that of the undelayed system up to an airspeed of 53.5m/s. In this case however, period doubling-behaviour does not take place. Instead, the high amplitude period-1 limit cycle behaviour continues up to an airspeed of just over 54 m/s when the system begins to flutter.

Consequently, unlike the bilinear and freeplay cases, delayed feedback increases the stability of the backlash system by delaying flutter. This phenomenon is due to the nature of the backlash function itself. When the control surface pitch displacement changes direction, the direction of the delayed displacement feedback is still unchanged and therefore the backlash region of figure 5 is shrunk, thus diminishing the effect of the nonlinearity.

Airspeed (m/s)	Stability
< 44	Stable
44-52.5	Low amplitude Period-1 Limit Cycle
> 54.3	Unstable (flutter)

Table 10: Stability of freeplay system with delayed feedback

4.4 Stability of system with control surface pitch limit

The nonlinear function described by the control scheme presented in section 2.6 is shown in figure 19. The feedback signal is zero unless the linear extrapolation of β, the control surface pitch degree of freedom, suggests that the value of β in the next step will be higher than the defined pitch limit, in which case the feedback signal is equal to $-a\beta$ where a is a gain coefficient. Consequently, it is obvious that, if the pitch limit were equal to zero, then the control law would be a linear proportional feedback. For the purposes of this work, the limit was set to $\pm 10^{\circ}$.

The effectiveness of the control scheme is demonstrated in figure 20 where the control surface pitch is plotted against time. The dashed line is the demand signal fed to the control surface through the power control unit. It can be seen that pitch rarely exceeds the limit of 10°, even though the demand angle is 12°.

Since the control system only engages when the control surface pitch lies near the limit, it does not affect the decaying impulse response of the system. Hence, self-excited oscillations are only possible when the linear system flutters. In other words, the control system contains flutter by constraining the system response onto a limit cycle. This can be seen in figure 21 where the bifurcation diagram for the pitch limited system is shown. Up to 52.7m/s, the flutter speed of the linear system, the response is decaying. Limit cycles exist at airspeeds between 52.7m/s and 57.7m/s. Beyond this range, the closed-loop system flutters.

Airspeed (m/s)	Stability
< 52.7	Stable
52.7-57.7	Period-3 Limit Cycle
> 57.7	Unstable (flutter)

Table 11: Stability of system with control surface pitch limit

It can be seen from the figure that the limit cycles are very complex since many points appear at each airspeed, in fact so many that it is impossible to classify the limit cycles in terms of period. A phase-space plot of a limit cycle at an airspeed of 55m/s is shown in figure 22. The complicated shape of the limit cycles is due to the simplistic manner in which the value of the control surface pitch

at the next time step is calculated. A more detailed prediction algorithm would give rise to better behaved limit cycles but would be less realistic.

4.5 Stability of system with friction in the PCU

Friction is a mechanism that removes energy from the motion of a system. Given that the amplitude of the frictional force, F_R, is low enough not to cause stoppages, its main effect is to increase the damping present in the motion. A frictional force of varying amplitude was added to the open-loop linear, freeplay and bilinear systems. As was expected, the main consequence for all the systems was an increase in damping. This effect can be observed in figures 23 and 24 where the control surface pitch impulse response of the frictionless linear system is plotted on the same axes as that of the system with friction. In figure 23, showing impulse responses at a subcritical airspeed (V=30m/s), the response of the frictional system dies away 0.35 seconds after the application of the impulse while the frictionless system still oscillates visibly after one second. Figure 24 shows impulse responses at an airspeed very close to the flutter speed of the linear system. In this case, the response of the system with friction takes a little longer to die away but its motion looks still far more damped than that of the frictionless system.

Nevertheless, friction does not alter the stability of any of the systems investigated in this work. The flutter speeds of the linear, bilinear and freeplay systems are not affected by the introduction of friction when F_R is low enough not to cause stoppages. Additionally, the limit cycle amplitudes of the bilinear and freeplay system also remain unaffected. However, when F_R exceeds a certain level, stoppages in the motion occur and the stability of all the systems is affected dramatically. Figure 25 shows the variation of flutter airspeed for the freeplay and bilinear systems with friction of increasing amplitude. In both cases, the flutter speeds remain at their respective frictionless values until $F_R = 1.4$N. At that particular value, the friction starts to cause stoppages and the LCOs that would have occurred in the absence of friction are inhibited. Additionally, the flutter speed is increased and keeps increasing at even higher values of F_R. The response of the bilinear system with friction of amplitude $F_R = 2$N is compared to that of the frictionless bilinear system in figure 26. It can be seen that, in the absence of friction, the system undergoes limit cycle oscillations. Friction suppresses the LCO by inhibiting the motion to such an extent that only irregular, low-amplitude oscillations are possible.

5 Conclusions

A simple aeroservoelastic system has been used to explore the effect of nonlinearities on the aeroservoelastic behaviour. It was found that it is possible for Limit Cycle Oscillations to occur, which may be of high period. The linear feedback that was applied still helped to stabilise the system, even with the presence of nonlinearities. Delays in the feedback signals reduced the effectiveness of the control in all systems apart from the system with backlash. If this delay was too great, then instability occurred almost immediately. A nonlinear control law designed to limit the control surface pitch response was found to increase the flutter speed considerably by forcing the system to undergo limit cycle oscillations instead. Friction was not found to alter the stability of any of the systems investigated here as long as its amplitude was low enough not to cause stoppages in the motion.

References

[1] D. S. Woolston, H. L. Runyan, and T. A. Byrdsong. Some effects of system nonlinearities in the problem of aircraft flutter. Technical Note TN 3539, NASA, October 1955.

[2] E. Breitbach. Effects of structural nonlinearities on aircraft vibration and testing. Technical Report AGARD-R-665, AGARD, January 1978.

[3] J. E. Cooper and T. T. Noll. Technical evaluation report on the 1995 specialists' meeting on advanced aeroservoelastic testing and data analysis. In *AGARD-CP-566*, May 1995.

[4] AGARD report 822. Numerical unsteady aerodynamic and aeroelastic simulation, May 1998.

[5] M. Holden, R. E. J. Brazier, and A. A. Cal. Effects of structural non-linearities on a tailplane flutter model. In *International Forum on Aeroelasticity and Structural Dynamics*, Manchester, UK, 1995.

[6] M. D. Conner, D. M. Tang, E. H. Dowell, and L.N. Virgin. Nonlinear behaviour of a typical airfoil section with control surface freeplay: a numerical and experimental study. *Journal of Fluids and Structures*, 11:89–109, 1997.

[7] S. H. Kim and I. Lee. Aeroelastic analysis of a flexible airfoil with a freeplay non-linearity. *Journal of Sound and Vibration*, 193(4):823–846, 1996.

[8] I. Lee and S. H. Kim. Aeroelastic analysis of a flexible control surface with structural nonlinearity. *Journal of Aircraft*, 32(4):869–874, 1995.

[9] S. J. Price, B. H. K. Lee, and H. Alighanbari. Postinstability behaviour of a two-dimensional airfoil with a structural nonlinearity. *Journal of Aircraft*, 31(6):1395–1401, 1994.

[10] S. J. Price, H. Alighanbari, and B. H. K. Lee. The aeroelastic behaviour of a two-dimensional airfoil with bilinear and cubic structural nonlinearities. *Journal of Fluids and Structures*, 9:175–193, 1995.

[11] F. Mastroddi and L. Morino. Limit-cycle taming by nonlinear control with applications to flutter. *Aeronautical Journal*, pages 389–396, November 1996.

[12] G. Dimitriadis and J. E. Cooper. Limit cycle oscillation control and suppression. *Aeronautical Journal*, pages 257–263, May 1999.

[13] S. A. Morton and P. S. Beran. Hopf bifurcation analysis of airfoil flutter at transonic speeds. *Journal of Aircraft*, 36(2):421–429, 1999.

[14] H. Zimmermann. Aeroservoelasticity. *Computer Methods in Applied Mechanics and Engineering*, 90:719–735, 1991.

[15] J. Becker and V. Vaccaro. Aeroservoelastic design, test verification and clearance of an advanced flight control system. In *AGARD-CP-566*, May 1995.

[16] G. J. Hancock, J. R. Wright, and A. Simpson. On the teaching of the principles of wing flexure-torsion flutter. *Aeronautical Journal*, pages 285–305, October 1985.

[17] W. G. Luber. Flutter prediction on a combat aircraft involving backlash and actuator failures on control surfaces. In *Proceedings of the International Forum on Aeroelasticity and structural dynamics*, Manchester, UK, May 1995.

[18] Z. C. Yang and L. C. Zhao. Analysis of limit cycle flutter of an airfoil in incompressible flow. *Journal of Sound and Vibration*, 123(1):1–13, 1988.

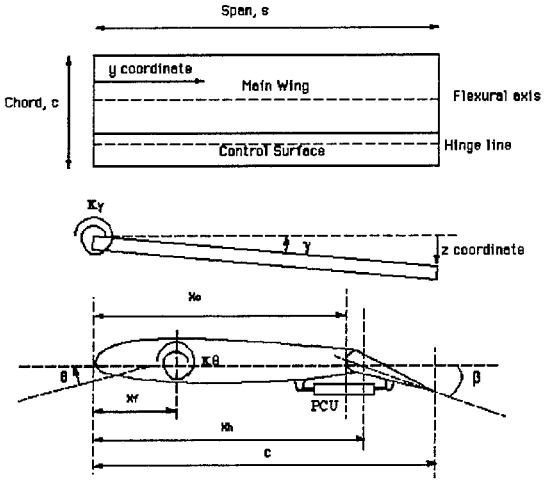

Figure 1: Basic Hancock model with control surface and PCU

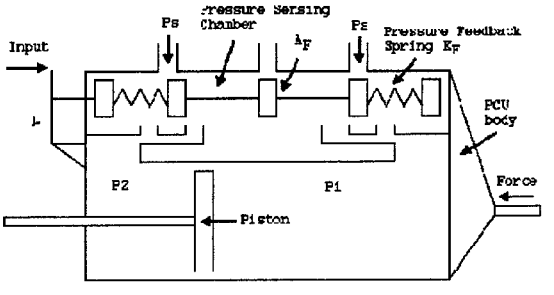

Figure 2: Power Control Unit

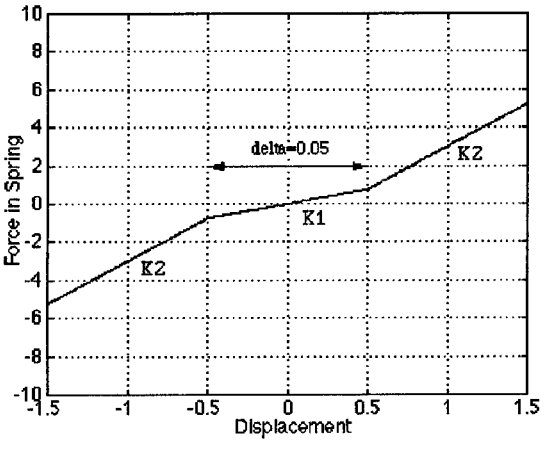

Figure 3: Bilinear stiffness vs displacement

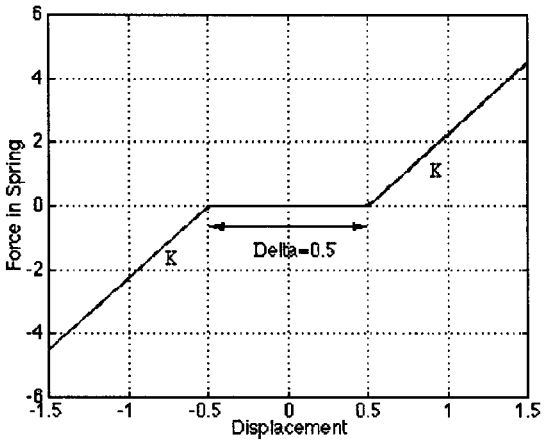

Figure 4: Freeplay stiffness vs displacement

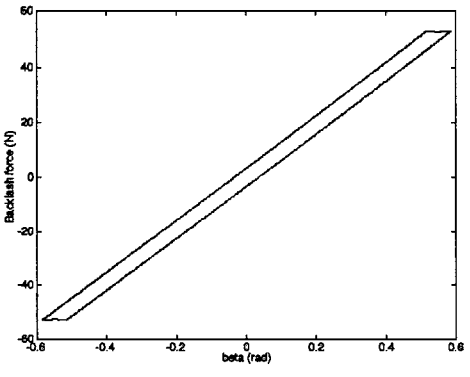

Figure 5: Backlash stiffness vs displacement

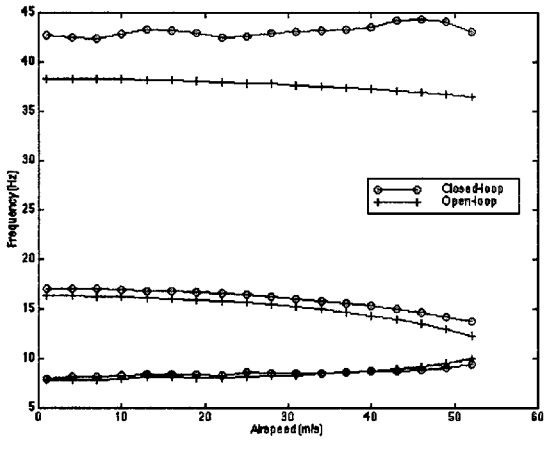

Figure 6: Open and closed loop natural frequencies of linear system

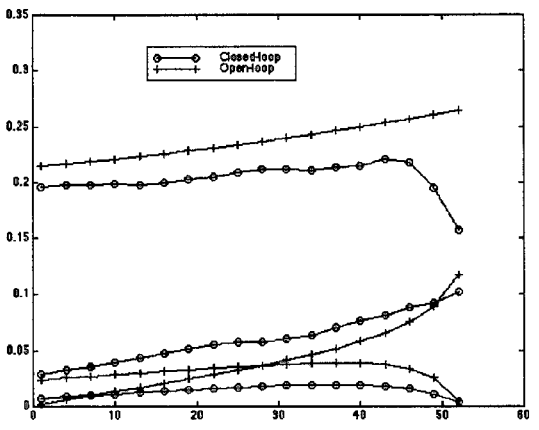

Figure 7: Open and closed loop damping ratios of linear system

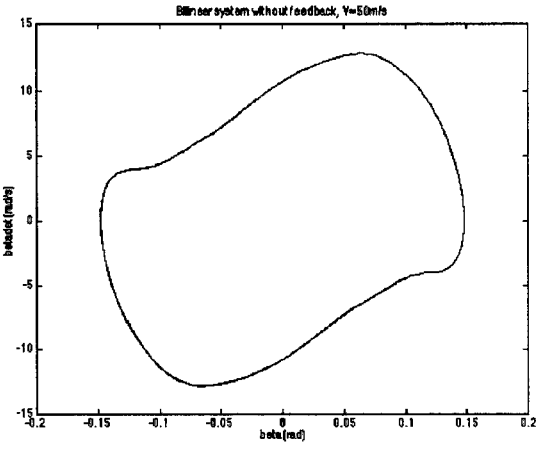

Figure 8: Phase-space diagram of period-1 limit cycle

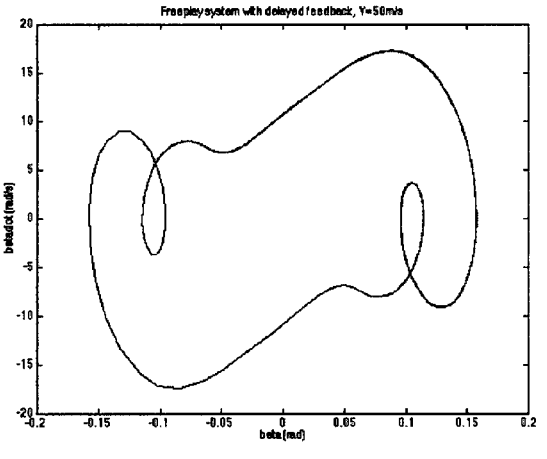

Figure 9: Phase-space diagram of period-3 limit cycle

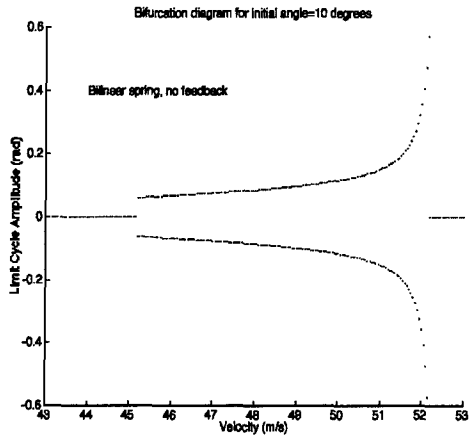

Figure 10: Bifurcation diagram of system with bilinear spring, no feedback

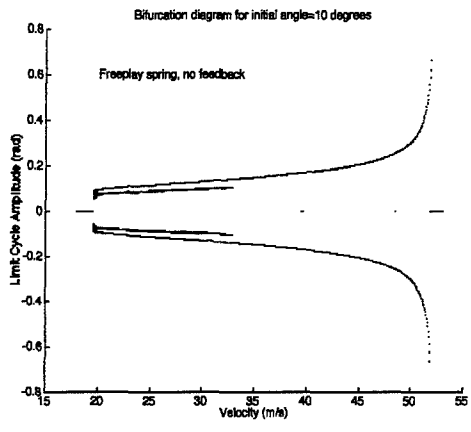

Figure 13: Bifurcation diagram of system with freeplay spring, no feedback

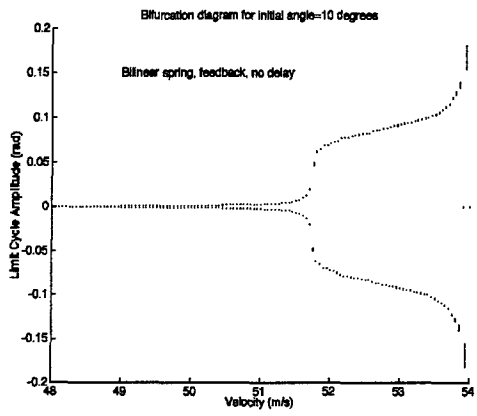

Figure 11: Bifurcation diagram of system with bilinear spring and feedback, no delay

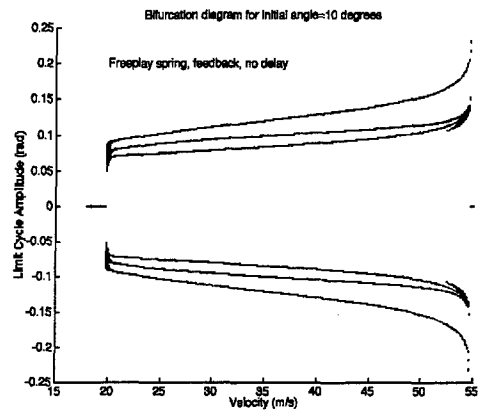

Figure 14: Bifurcation diagram of system with freeplay spring and feedback, no delay

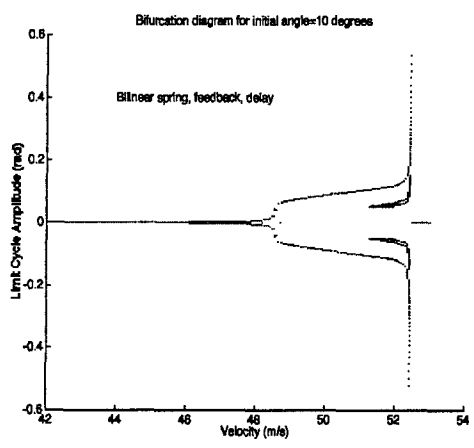

Figure 12: Bifurcation diagram of system with bilinear spring, feedback and delay

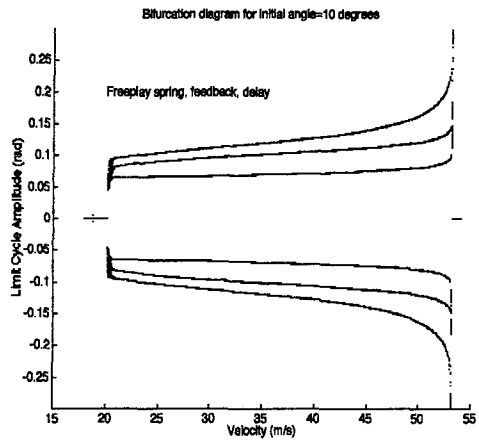

Figure 15: Bifurcation diagram of system with freeplay spring, feedback and delay

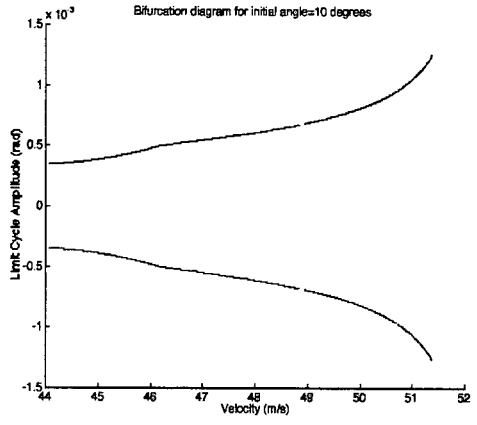

Figure 16: Bifurcation diagram of system with backlash, no feedback

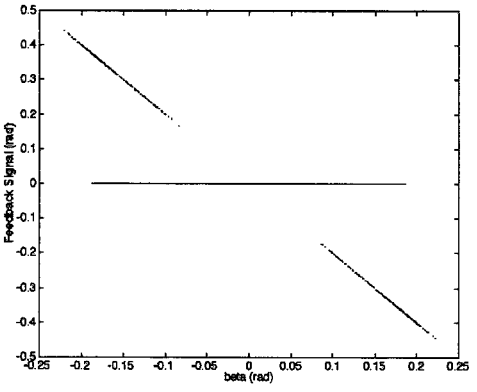

Figure 19: Nonlinear function of control surface pitch limiting control scheme

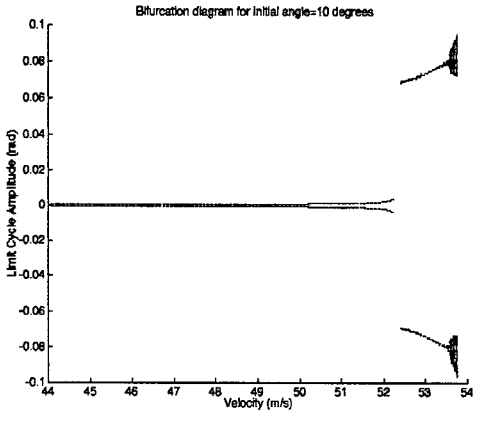

Figure 17: Bifurcation diagram of system with backlash and feedback, no delay

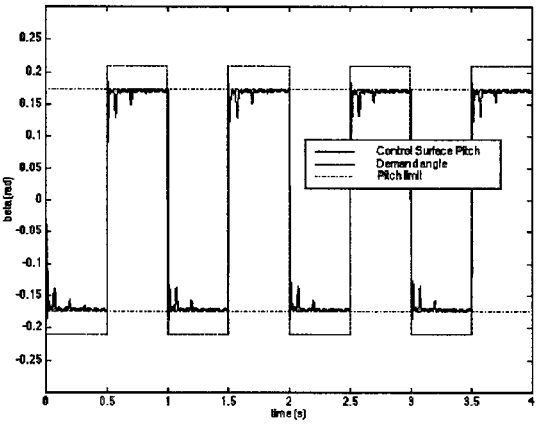

Figure 20: Performance of control surface pitch limiting control scheme

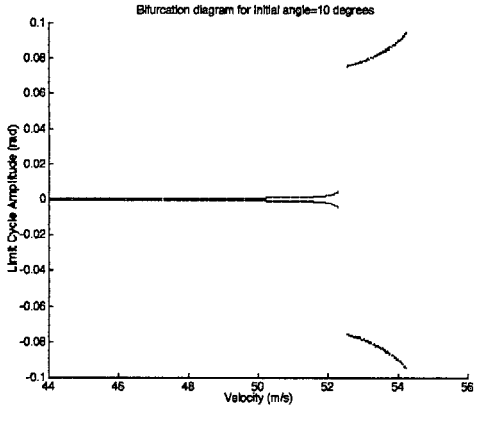

Figure 18: Bifurcation diagram of system with backlash, feedback and delay

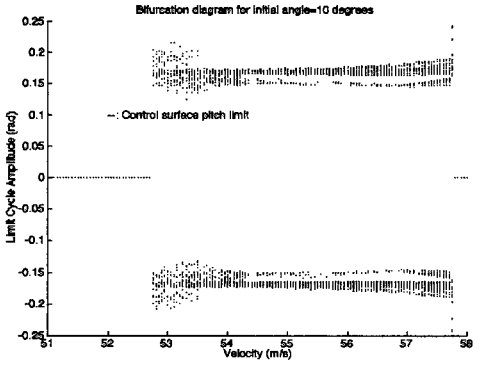

Figure 21: Bifurcation diagram of system with control surface pitch limit

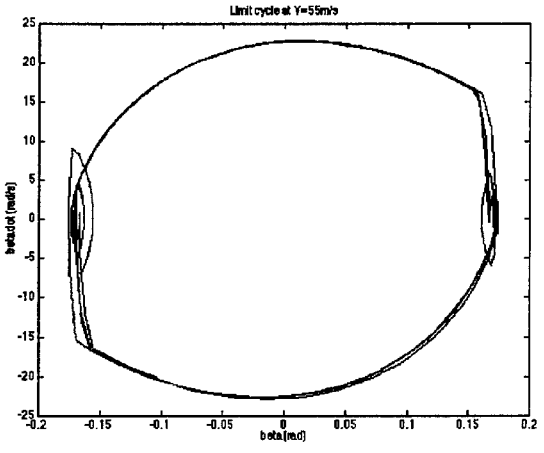

Figure 22: Limit cycle of system with control surface pitch limit at V=55m/s

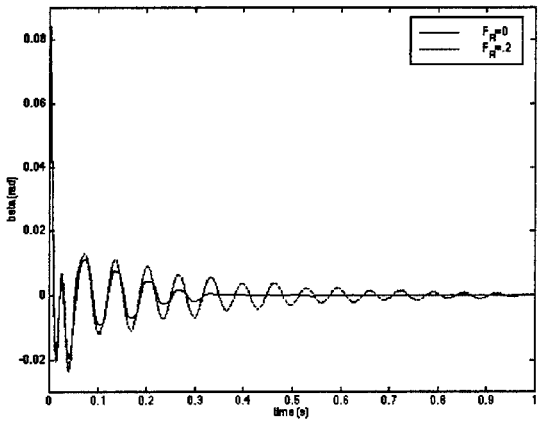

Figure 23: Comparison of responses of frictionless system and system with friction at V=30m/s

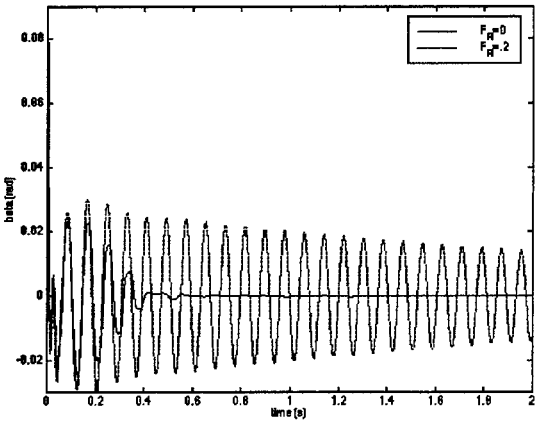

Figure 24: Comparison of responses of frictionless system and system with friction at V=52m/s

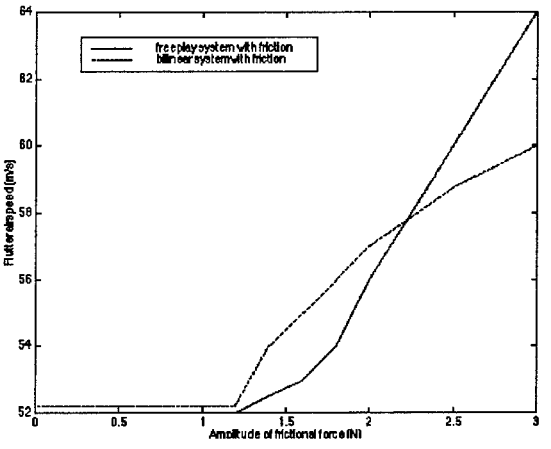

Figure 25: Variation of flutter speed of bilinear and freeplay systems with increasing frictional amplitude

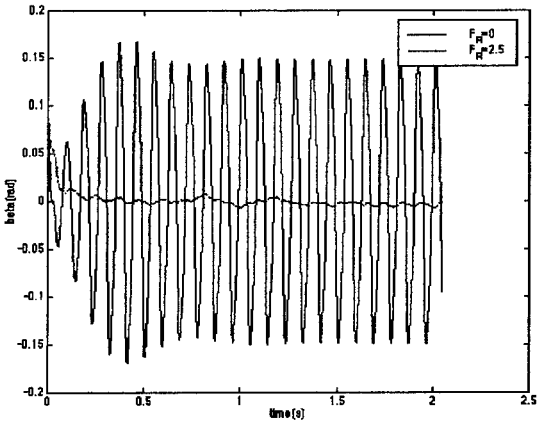

Figure 26: Comparison of responses of bilinear system with and without friction at V=50m/s